Mechanism of Electric-Pulse-Induced Resistance Switching in Manganites

M. Quintero,[1,2] P. Levy,[1] A. G. Leyva,[1,2] and M. J. Rozenberg[3,4]

[1]*Departamento de Física, CAC, CNEA, Av. Gral Paz 1499, Buenos Aires (1650), Argentina*
[2]*Escuela de Ciencia y Tecnología, UNSAM, San Martín, Buenos Aires (1650), Argentina*
[3]*Laboratoire de Physique des Solides, CNRS-UMR8502, Universite de Paris-Sud, Orsay 91405, France*
[4]*Departamento de Física, FCEN, Universidad de Buenos Aires, Ciudad Universitaria Pab.I, Buenos Aires (1428), Argentina*

(Received 20 April 2006; published 12 March 2007)

We investigate the electric-pulse-induced resistance switching in manganite systems. We find a ''complementarity'' effect where the contact resistance of electrodes at opposite ends show variations of opposite sign and is reversible. The temperature dependence of the magnitude of the effect reveals a dramatic enhancement at a temperature T^*, below the metal-insulator transition. We qualitatively capture these features with a theoretical model, providing evidence for the physical mechanism of the resistance switching. We argue that doping control of the electronic state of the oxide at the interfaces is the mechanism driving the effect.

DOI: 10.1103/PhysRevLett.98.116601 PACS numbers: 72.80.Ga, 72.15.Gd, 72.20.−i, 73.40.Rw

There is increasing interest in the investigation of transition-metal oxides (TMO) as candidate materials for novel electronic devices such as nonvolatile random access memories. The phenomena of nonvolatile resistance switching (RS), the sudden change of the resistance by the application of a strong electric field [1], is a research field that is experiencing a burst of activity [2]. The main driving force is the potential application in next generation electronic memory devices. Nevertheless, from a fundamental research perspective, interesting questions also emerge. For instance, the understanding of the transport properties of TMOs under the extreme conditions of high electric fields that bring the material to the verge of the dielectric breakdown, and the possible relevance of strong correlation effects. The simplest device that displays the RS effect amounts to two metallic electrodes separated by a dielectric, in a capacitorlike structure. The metal contacts can be ordinary metals such as Ag, Pt, Al, etc., and the dielectric might be any from a wide variety of TMOs. Quite surprisingly in fact, the RS effect is ubiquitous in TMO. It has already been reported in a very large number of systems, ranging from simple binary oxides such as CeO_2, Y_2O_3, ZrO_2, TiO_2 [3–6], and the classic Mott insulators NiO and Fe_2O_3 [7], to complex perovskites [8], including cuprates such as La_2CuO_4 [9] and $Bi_2Sr_2CaCu_2O_{8+y}$ [10]. Among the first materials to be systematically investigated we note the Ca doped manganites [11–14], already popular due to their colossal magnetoresistance [15–17]. The universal observation of RS in TMOs may suggest a unique underlying physical mechanism, but despite its technological promise, the origin of the effect remains largely not understood.

We focus on the physical origin of the RS phenomena in perovskite manganites where room temperature RS has already been reported [18]. We perform two experiments that provide key clues on the physical nature of the effect: first, we characterize the RS in the two interfaces of the system; and second, we measure the RS change as a function of the temperature. These two experiments are then contrasted to the predictions of a theoretical model [19,20]. The good qualitative agreement allows us to argue that the physical mechanism driving the resistance switching in perovskite manganites is likely to be doping control of the electronic state of the dielectric oxide at the contact interfaces. In this work we study several bulk polycrystalline samples of $Pr_yLa_{0.375-y}Ca_{0.325}MnO_3$ (PLCMO) with $y = 0.3$ and 0.32, and average grain size 2 μm. Four similar contacts were hand painted with silver paste on top of the specimen, each one at some fraction of a millimeter apart from the other. To induce a resistance change, a train of pulses of a given polarity is applied to the electrodes at opposite ends, A and D (see Fig. 1). Then, the effect can be reversed by changing the polarity of the train. Positive pulses are defined as those setting terminal D at a

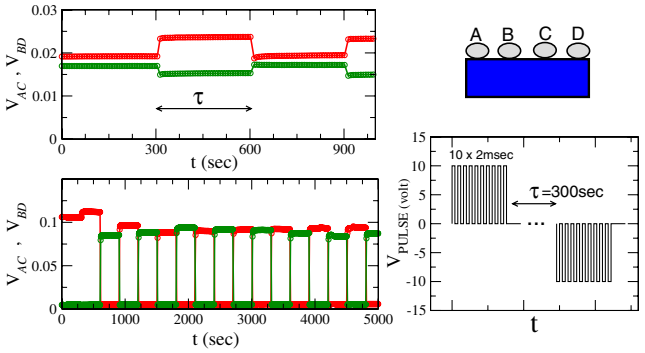

FIG. 1 (color online). Top left: Room temperature interfacial voltage (in volts) at V_{AC} (red) and V_{BD} (green) as a function of time for a $y = 0.32$ sample. Bottom left: Idem, for a $y = 0.3$ sample. Top right: Schematic electrode configuration. Bottom right: Schematic voltage protocol applied at terminals A and D (trains of 10 pulses of amplitude ± 10 V, duration 2 ms, separation 2 ms, $I_{PROT} = 400$ mA).

higher potential than terminal A. The trains are applied at intervals $\tau = 300$ sec. During the intervals, we measure the voltage difference at terminals AC, BD, and BC under a constant and small bias current injected through the opposite end terminals A and D (unless otherwise stated, $I_{\text{bias}} = 1$ mA). We used a source-meter Keithley 2400 in voltage control mode, setting the limit for current flow at I_{PROT}. At a constant bias current, the potential drop at BC is proportional to the intrinsic bulk resistivity of the sample. In contrast, by means of a three-lead configuration, the potential drops either at AC or BD measure the sum of intrinsic plus interfacial resistance at the respective electrode-manganite contact. The comparison of voltage drops in each configuration indicates that the resistance of the interfaces is much larger than the bulk contribution.

Figure 1 shows V_{AC} and V_{BD} as a function of time that independently and simultaneously sense the interfacial voltage drop at the opposite pulsed electrodes, A and D. The observed switching of V_{AC} and V_{BD} between high resistance (HR) and low resistance (LR) states is stable, showing nonvolatility in qualitative agreement with previous reports in the literature [8,12]. The stability of states over several hours was confirmed. Many samples were measured and a large sample-to-sample variation of the magnitude of the effect was observed. The two sets of data shown in the figure illustrate both a case where one of the largest on-off ratio ($R_{\text{HR}}/R_{\text{LR}}$) was obtained and also a typical case with a more modest effect. Nevertheless, a most remarkable and universal feature observed in the totality of samples studied is a ''complementary'' character of the switching at interfaces of opposite ends. By complementary we mean that upon application of a train of a given polarity, one interface increases its resistance while the other decreases it. Then, the next train of opposite polarity reverses the effect at both interfaces simultaneously. In addition, we observed that regardless of the value of the ratio, the size of the resistance change at the two interfaces was almost always of the same order magnitude.

To gain further insight in the nature of the physical mechanism of RS we measured its temperature dependence. We vary T from 25 K to room temperature, crossing a known metal-insulator transition at T_C [17]. Insets of Fig. 2 show the nonmonotonic $V_{BC}(T)$ (proportional to the bulk resistivity) displaying the transition in two samples of different composition. To quantify the strength of the resistance switching we adopt the definition $\text{RS} = (R_{\text{HR}} - R_{\text{LR}})/R_{\text{AV}}$, where the average resistance $R_{\text{AV}} = (R_{\text{HR}} + R_{\text{LR}})/2$. Thus, RS can vary between 0 and 2. Figure 2 shows RS(T) for two samples ($y = 0.3$ and 0.32). While their respective values of RS(T) are different, the results are qualitatively consistent both showing a dramatic enhancement of at a temperature T^*, lower than T_C. The maximum in RS(T) at T^* seems correlated with the rapid increase of the bulk resistivity with T.

We shall now turn to our model calculations to try to qualitatively capture the phenomena described before. Our

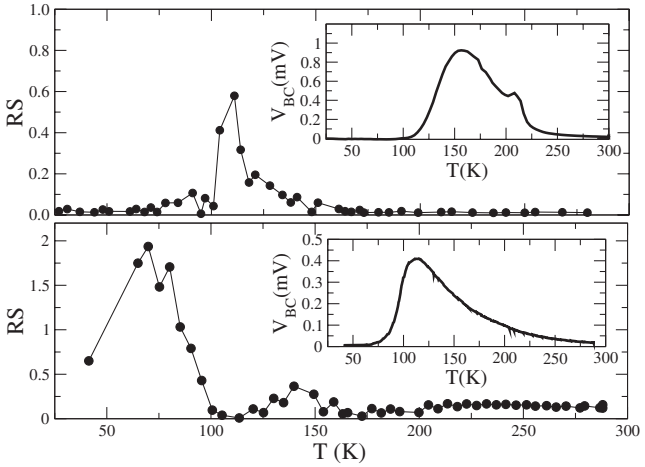

FIG. 2. Resistance switching as a function of temperature. Top panel is for a sample of $y = 0.3$ (measured at $I_{\text{bias}} = 0.1$ mA), and the bottom one is for the same sample of Fig. 1 of $y = 0.32$. The maximum in the RS(T) occurs at T^*. The inset of the panels show the respective V_{BC} (proportional to bulk resistivity); the maximum corresponds to T_C, the metal-insualtor transition.

starting point is a phenomenological model that was recently introduced [19,20]. In its original formulation the model postulates the existence of a network of spatial inhomogeneities within the dielectric material (called domains), and that carriers hop from one domain to another under the action of an applied electric field. Note that the assumption of spatial inhomogeneities is sound for TMOs in general [16], and certainly well justified in the present case of manganites [21], where phase separation in PLCMO was observed in a wide temperature range [17]. As is schematically shown in Fig. 3, the inhomogeneities in the dielectric that are in physical proximity to the contacts are explicitly modeled by two sets of small domains neighboring the electrodes (called top and bottom). In addition, the inhomogeneities in the bulk are inexplicitly lumped onto a single central large domain. These bulk inhomogeneities might correspond, for instance, to filamentary conduction paths across the sample that provide a bridge between the interfaces. Upon application of a voltage to the electrodes, carriers move across the system by hopping through the domains. This model captures some basic phenomenology of resistive switching, including the nonvolatility of the resistive states.

In the present case, we shall build on this phenomenological model just described and extend it along the following ideas. We first identify the mobile carriers of the model with the defects of the dielectric, more precisely, with oxygen vacancies as suggested by recent experiments [22]. Evidently, electric conduction is not mediated by oxygen vacancies, thus the model is merely thought to describe how the concentration of these defects is affected in the bulk dielectric (large domain) and near the interfaces (small domains) by the strong electric pulsing. The oxygen concentration in manganites, as in most other TMOs, is a

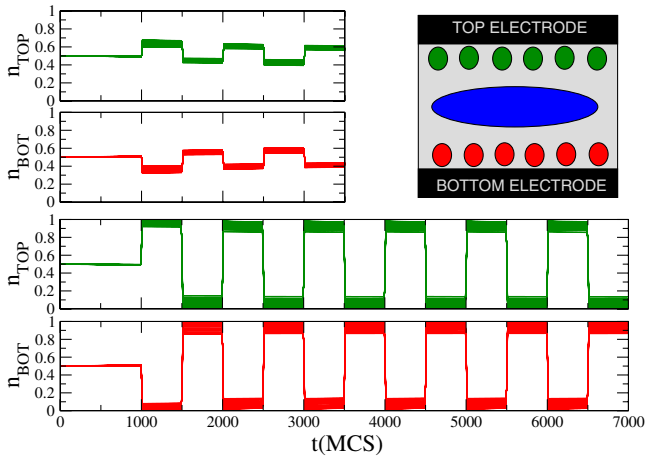

FIG. 3 (color online). Model results for the occupation level of the small interfacial domains (top in green and bottom in red), under the action of a protocol of individual voltage pulses of alternate polarity. Pulses are applied every 500 Monte Carlo time steps (MCS), have a duration of 10 mcs, and the first pulse is at 1000 MCS. The model parameters are $\Gamma_{\text{elect-domain}} = 10^{-15}$ and $\Gamma_{\text{domain-domain}} = 0.3 \times 10^{-15}$, all other model parameters are as those in Ref. [19]. In each panel there are 40 green or 40 red lines (cannot be resolved) for an equal number of top and bottom domains. The upper (left) panel corresponds to applied pulses of strength $V = 4.5$ (in arbitrary units). The lower one is for $V = 6.5$ that shows saturation. Top right: Domain model.

key parameter to control the transport properties. Thus the spatial modulation of oxygen vacancy concentration will imply a modulation of the resistivity across the system. To make further progress, we need to explicitly relate the local oxygen concentration (i.e., local doping) to the local resistivity of the system. The qualitative physics of these compounds is captured by the "double exchange" (DE) Hamiltonian [15,23]. We shall thus adopt it here to obtain the dependence of the resistivity with temperature and doping level.

Our calculations will proceed in two stages: First we shall show that the domain model naturally predicts the complementarity effect, by producing opposite variations of the oxygen concentration at opposite electrodes. Then, we shall show that if one admits that the RS originates from a variation of resistivity due to a variation of oxygen content at the interfaces, the predictions from the DE Hamiltonian qualitatively describe the peculiar temperature behavior of the experimental results.

Figure 3 shows the results of Monte Carlo calculations using the domain model similarly as in Ref. [19]. The plots present the model predictions for the variation of the concentration of oxygen vacancies near the interfaces (i.e., occupation the small domains). As suggested by the experimental system, we adopt a symmetric choice of the phenomenological parameters Γ that control the probabilities for particle transfers between domains (see figure caption). What one basically observes in the figure is that, under the action of alternative pulsing, oxygen vacancies move back and forth between the central region and the small interfacial domains. The latter are thus filled up and emptied with the alternative pulsing in a complementary manner. The magnitude of the effect is mainly controlled by the intensity of the applied external voltage.

To fully theoretically underpin the idea of oxygen doping control of the electronic state of the dielectric at the interfaces we adopt the DE Hamiltonian that reads,

$$H_{\text{DE}} = \sum_{\langle ij\rangle\sigma} t c^{+}_{\sigma i} c^{\dagger}_{\sigma j} + \sum_{i} J S_i s_i, \tag{1}$$

where the sum is over nearest-neighbor sites and the operators $\{c_i^{+}, c_i\}$ represent the electrons of the e_g conduction band of bandwidth proportional to the hopping t. The units are set by $t = 1$, in manganites $t \sim 1$ eV [15,23]. The electron spin density s_i is coupled to the local classic spins S_i with a ferromagnetic interaction J. The local spins describe the three localized and Hund's coupled t_{2g} electrons at every lattice site. For simplicity we consider the S_i as Ising spins. The occupation of the band is adjusted with the chemical potential, and from the nominal chemical composition one would expect that the electron density $n \approx 0.675$, i.e., the doping $\delta = 1 - n \approx 0.325$. Following previous work on the DE Hamiltonian we set $J/t = 4$, thus there are no free parameters left. We solve for the DE Hamiltonian using the dynamical mean field theory technique [24], as originally done by Furukawa [23]. We calculate the dc resistivity using the Drude formula, where the relaxation time is estimated from the low frequency behavior of the electron self-energy. The results for the resistivity ρ as a function of temperature and carrier doping δ are shown in Fig. 4 (left panel). One can see that this Hamiltonian qualitatively captures the metal-insulator transition producing a maximum of $\rho(T)$ at T_C for each doping value.

The resistivity displays a strong dependence on the doping level, which is usually the case for strongly corre-

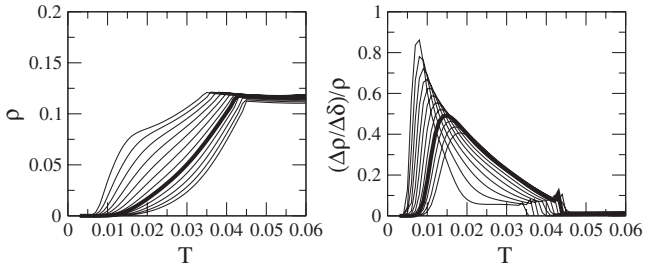

FIG. 4. Left: Resistivity ρ as a function of T for different doping δ calculated using the double exchange Hamiltonian. The doping δ is from 0.16 to 0.40 with step 0.02 (left to right), $\delta = 0.3$ is in thick line. Right: Relative variation of the resistivity with doping $[1/\rho(\delta, T)][\Delta\rho/\Delta\delta]$ (same δ values, increasing to the right). This quantity can be directly compared to the experimental RS results (see text).

lated systems. It is important to note that the decrease of the resistivity with doping δ is consistent with the experimental observation that the negatively pulsed electrode (that attracts positively charged oxygen vacancies) lowers its resistance. Based on the previous discussion, we assume that pulsing produces small changes of the local concentration of oxygen vacancies (i.e., of doping) at the dielectric side of the contact interfaces. More precisely, the positively (negatively) pulsed electrode would increment (decrease) the oxygen vacancy concentration at the dielectric interface. Therefore, we can estimate the prediction for the RS(T) from the variation of the resistivity with respect to doping and normalizing by the resistivity $\frac{1}{\rho(\delta)}\frac{\Delta\rho}{\Delta\delta}$. This quantity should be directly proportional to the experimental definition of the RS strength $(R_{\mathrm{HR}} - R_{\mathrm{LR}})/(R_{\mathrm{AV}})$. In the right panel of Fig. 4 we show the results RS(T) from the DE Hamiltonian calculation in a range of doping values. In qualitative agreement with the experimental case (Fig. 2), the RS(T) shows a dramatic enhancement in the region where the resistivity shows a fast increase, below the metal-insulator transition.

In conclusion, our experimental and theoretical study of the resistance switching effect in manganites provides strong evidence that the physical origin is the doping control of the electronic state of the dielectric at the interfaces, by inducing local changes of oxygen vacancy concentration with electric pulsing. An important point that needs to be emphasized is that, according to our study, a key ingredient for RS phenomena is a strong variation of the dielectric resistivity with doping (i.e., concentration of oxygen defects). This feature is typical of strongly correlated systems such as transition-metal oxides where the nature of the $3d$ orbitals leads to a competition between the itinerancy and localization tendencies. This observation may provide important clues to understand the perplexing universality of the resistance switching effect that is actually seen in a large variety of transition-metal oxides.

We thank R. Weht for valuable help and discussions. Research partially supported by ANPCyT PICT Nos. 03-13517 and 03-11609, PICS CNRS-SECYT, and ECOS-Sud.

[1] G. Dearnaley, A. M. Stoneham, and D. V. Morgan, Rep. Prog. Phys. **33**, 1129 (1970); H. Pagnia and N. Sotnik, Phys. Status Solidi A **108**, 11 (1988).
[2] Y. Tokura, Phys. Today **56**, No. 7, 50 (2003); W. W. Zhuang *et al.*, in *International Electron Devices Meeting*, Technical Digest No. 02CH37358 (IEEE, Piscataway, NJ, 2002), p. 193 196; A. Beck, J. G. Bednorz, Ch. Gerber, C. Rossel, and D. Widmer, Appl. Phys. Lett. **77**, 139 (2000).
[3] R. Fors, S. I. Khartsev, and A. M. Grishin, Phys. Rev. B **71**, 045305 (2005).
[4] A. L. Pergament, V. P. Malinenko, O. I. Tulubaeva, and L. A. Aleshina, Phys. Status Solidi A **201**, 1543 (2004).
[5] S. Kim *et al.*, Jpn. J. Appl. Phys. **44**, L345 (2005).
[6] B. J. Choi *et al.*, J. Appl. Phys. **98**, 033715 (2005).
[7] S. Seo *et al.*, Appl. Phys. Lett. **85**, 5655 (2004).
[8] S. Tsui *et al.*, Appl. Phys. Lett. **85**, 317 (2004).
[9] A. Sawa, T. Fujii, M. Kawasaki, and Y. Tokura, Jpn. J. Appl. Phys. **44**, L1241 (2005).
[10] N. A. Tulina, A. M. Lonov, and A. N. Chaika, Physica (Amsterdam) **C366**, 23 (2001).
[11] S. Q. Liu, N. J. Wu, and A. Ignatiev, Appl. Phys. Lett. **76**, 2749 (2000); X. Chen, N. J. Wu, J. Strozier, and A. Ignatiev, Appl. Phys. Lett. **87**, 233506 (2005).
[12] A. Baikalov *et al.*, Appl. Phys. Lett. **83**, 957 (2003).
[13] A. Odagawa, H. Sato, I. H. Inoue, H. Akoh, M. Kawasaki, and Y. Tokura, Phys. Rev. B **70**, 224403 (2004).
[14] R. Dong *et al.*, Appl. Phys. Lett. **86**, 98 (2005); T. L. Chen *et al.*, Thin Solid Films **488**, 167 (2005).
[15] E. Dagotto, *Nanoscale Phase Separation and Colossal Magnetoresistance*, The Physics of Manganites and Related Compounds (Springer, New York, 2002).
[16] E. Dagotto, Science **309**, 257 (2005).
[17] M. Uehara *et al.* Nature (London) **399**, 560 (1999).
[18] M. Quintero, A. G. Leyva, and P. Levy, Appl. Phys. Lett. **86**, 242102 (2005).
[19] M. J. Rozenberg, I. H. Inoue, and M. J. Sánchez, Phys. Rev. Lett. **92**, 178302 (2004).
[20] M. J. Rozenberg, I. H. Inoue, and M. J. Sánchez, Appl. Phys. Lett. **88**, 033510 (2006).
[21] T. Becker *et al.*, Phys. Rev. Lett. **89**, 237203 (2002).
[22] K. Szot, W. Speier, G. Bihlmayer, and R. Waser, Nat. Mater. **5**, 312 (2006).
[23] N. Furukawa, *Physics of Manganites*, edited by T. A. Kaplan and S. D. Mahanti (Plenum, New York, 1999).
[24] A. Georges, G. Kotliar, W. Krauth, and M. J. Rozenberg, Rev. Mod. Phys. **68**, 13 (1996).